

## Electrochemical Sensors and Determination for silver ion by Cyclic Voltammetry at iodine-coated Platinum nanoparticles electrode

Ahmad khalaf alkawaldeh<sup>1,2\*</sup>, Abdel Hadi Al Jafari<sup>1</sup>

<sup>1</sup> Department of Pharmaceutical Chemistry; College of Pharmacy, Jerash University, Jordan.

<sup>2</sup> Chemistry Department, The Hashemite University, P.O. Box 150459, Zarqa 13115, Jordan.

\* ah.alkawaldeh@jpu.edu.jo

### ABSTRACT

The platinum nanoparticle electrode, modified by iodine (PtNPs/I), was designed to simultaneously determine the use of Cyclic Voltammetry (CV) for silver ion. The analyzed maximum anodic peak current and maximum anodic potential were performed. The platinum nanoparticles deposited were characterized by electron dispersive X-ray spectroscopy (EDX), cyclic voltammetry and scanning electron microscope (SEM). The SEM micrograph shows that the size, shape, and homogeneity of platinum nanostructures are affected by deposition time and the frequency of the potential regime using the parameters  $E_i = -0.4V$ ,  $E_h = 0V$ ,  $dE/dT = 100$  mV/s, frequency of 100 Hz, 2 min deposition time and concentration of platinum solution  $10^{-4}$  M. The purpose of this work is to investigate the catalytic properties of the nanostructure platinum. It is found that the iodine monolayer was absorbed irreversibly to platinum nanostructured electrodes. Cyclic voltammetry experiments on iodine-coated platinum electrodes revealed their remarkable inertness to molecular adsorption, implying suppression of surface processes, interferences, and the overall current background in voltammetric measurements. Potentiostat adsorption of iodine at 0.20 V was used to create iodine-coated platinum electrodes. In 0.5M  $H_2SO_4$ , the passive potential window (working potential range) is approximately from -0.10 to 0.95 V. Voltammetric measurements of  $Ag^+$  on the iodine-coated electrode revealed a linear relationship between the anodic peak current and the silver ion bulk concentration. With a correlation coefficient of 0.993, the detection limit was  $6.8 \times 10^{-9}$  M.

### Keywords

Cyclic Voltammetry, Electrochemical Sensors, iodine-coated electrode, Platinum nanoparticles electrode, silver ion

### Introduction

The miniaturization trend for sensor platforms has led to a focus on electrochemical sensors micro/nanofabrication. Consequently, many recent electrochemical sensor publications focused on the development of micro-sensors, due to a range of factors including the potential for high spatial resolution [1-5]. Also included are the manufacturing and application of potential and voltammetric micro-sensors [6-8]. The microelectrode arrays maintain the main advantageous properties of single microelectrodes such as low-capacity current, making them more suitable with a higher sensitivity and improved signal-to-noise ratio for a majority of applications [9-11]. Due to their unique physical and chemical properties, such as a high surface to volume ratio, electrochemical sensor manufacturing still focuses on nanostructures including nanotubes and nanoparticles [12]. The nanostructures and the manufacture, physical and experimental characteristics of each material for use with these sensors are described [13, 14]. Use of nanoparticles in sensors focusing on catalysis, immobilization, electron transmission, bimolecular labeling, and reactants [15]. This last work has been focused on improvements in the biocompatibility and long-term stability of implantable electrochemical sensors [16, 17]. The two questions related to implantable chemical sensors and several strategies for improving the intravascular and subcutaneous sensor responses were discussed [18]. Developing electrochemical sensors to detect explosives, such as marine environments and gas-phase samples, has been reviewed. The electrochemistry sensor and sensor platforms of organic explosives including peroxide compounds and polynitroaromas [19]. Developments and uses for screen-printed electrodes including unmodified, foiled, enzyme-modifiable, and vaccine sensors [20]. The low cost and ease of production of printable materials led to a larger study of screen-prints, as demonstrated by the volume of recent publications [21]. Progress in the use of non-traditional electrode materials for electrochemical sensor production such as solid amalgam, carbon diamond and boron-doped diamonds [22]. Platinum electrodes with iodine-coated are of remarkable inert to molecular adsorption. This inertness of iodine-coated platinum electrodes was used to produce single-crystal platinum electrodes at atmospheric pressure [23, 24]. In addition, iodine-coated platinum electrodes are not oxygen-sensitive in aqueous solutions, unlike bare mercury and platinum electrodes. However, these electrodes respond to oxidation and reduction of ions [25]. The simplicity and durability of iodine-coated platinum electrodes are good candidates to replace the costly and demanding procedure involved in the production of mercury electrodes to measure ions [26].

During this work, the use in electrochemical sensor measurements for silver ions of iodine-coated platinum nanoparticles was examined.

## Experimental

### Instruments and Materials

A potentiostat (A273 Princeton Applied Research USA) interfaced to a computer through GPIB interface along with Echem® software was used for electronic control, cyclic voltammetry and linear scan experiments. The square wave with preset high and low values was generated from a function generator (Bk PRECISION, A 4003) and was fed to the potentiostat at the external input. The desired lower and higher limits of square wave values were obtained by adjusting the applied potential from the potentiostat. All reagents used were highly pure certified analytical reagent (A.R.) chemicals and used as received from the suppliers without further purification. The purging nitrogen was supplied by the National Gas Company and coupled with Oxisorb® cartridge (Suplico) to remove traces of oxygen. Reference electrode was an Ag/AgCl [KCl: 1.0 M]. The auxiliary electrode was made of platinum wire 0.2mm (99.99% purity, Aldrich chem.co, U.S.A). The working electrode was a tantalum Wire (99.95% pure, Good-fellow METALS, England), and the modified electrodes. Triply distilled water was used where the second distillation was carried out from basic potassium permanganate solution to get rid of any traces of organic impurities. Hexachloroplatinate solution ( $3.14 \times 10^{-3}$  M) was purchased from Janssen chemical, USA). The solution was originally (1mg/ml) platinum dissolved in 10% HCL solution. Iodine (Janssen, 98%, Belgium). Silver perchlorate hydrate from (99%, ACROS, USA). Sulfuric acid from (97%, Fluka, Germany). Hydrofluoric acid from (48%, Anala R, England). Nitric acid from (69%, Scharlau, Spain). Titanium metal from (99%, laboratory reagent, England).

### Cells and Electrodes

Deposition cell was used for electrodeposition of platinum nanostructures at the tantalum surface. The cell was a three-electrode cup cell. Another cell was an H-shape three-electrode cell, which was used for cyclic voltammetric measurements. The electrochemical cell was equipped with a multiple inlet and outlet system for admission of supporting electrolyte, purging and blanketing the solution with oxygen free nitrogen. The reference electrode was an Ag/AgCl and all the potentials reported in this thesis are referenced to this electrode.

### Experimental Procedures of Modification the Platinum nanoparticles electrode surface by Iodine

The platinum electrode was originally refined in a chromic acid solution that was recently prepared. The electrode was cycled between the evolution limit of hydrogen and oxygen (approximately -0.2 and 1.2 V) by the cycles until the clean platinum electrode reproduced its regular voltammograms. Modification of the platinum electrode surface was carried out by dipping the electrode into a solution that contains the cation of the element at open circuit conditions. Almost, in all cases, the concentration of the modifier ions was about  $1 \times 10^{-2}$  M and the dipping time was about 5 minute in cell. In such a case, the concentration of the cations equals the solubility of unit's salt in 0.5 M H<sub>2</sub>SO<sub>4</sub>. The cations that used for the modifications Iodine. The potential electrode was measured between the evolution limit for hydrogen (-0.1V) and the iodine oxidation threshold potential (approximately 0.95 V). The reproduction of voltammograms for the clean platinum nanoparticles electrode before any new experiment was conducted (Figure 1).

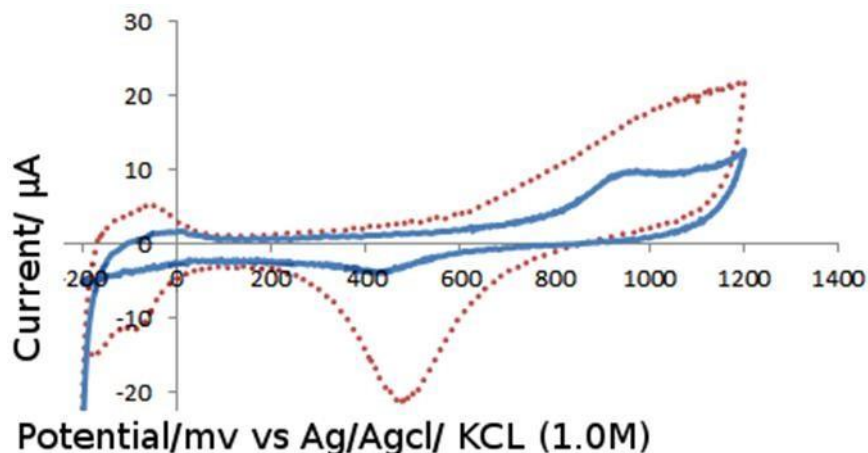


**Figure 1.** Voltammograms of platinum nanoparticle electrode (solid line) and polycrystalline platinum electrode (dashed line), at a scan rate of 100 mV/s.

## Results and Discussions

### Platinum nanostructures electrode

Square wave potential regimes were applied in different experimental conditions to figure out the optimal conditions for preparation of platinum nanostructured electrode on tantalum substrate. Experiment parameters:  $E_L = -0.4$ ,  $E_H = 0V$ , amplitude = 0.4V, frequency = 100 Hz, concentration =  $1 \times 10^{-4}$  M, time = 120 seconds and scan rate = 100 mV/s [24]. Figure 2 shows the SEM micrograph for platinum nanostructures on tantalum deposited from  $1 \times 10^{-4}$  M  $[PtCl_6^-]$  solution. The particles to a great extent are uniformly distributed on the surface. The calculated average of particles amounts to  $3.9 \times 10^{14}$  particle per  $cm^2$ . Figure 2 shows the voltammogram for the platinum nanostructured electrode deposited for 120 seconds. The SEM representative micrograph for platinum nanostructures produced by application of a square wave centered at -0.4 to 0V. The SEM micrographs shows that the platinum nanoparticles are same of size, shape and uniformity of distribution on the surface [27].

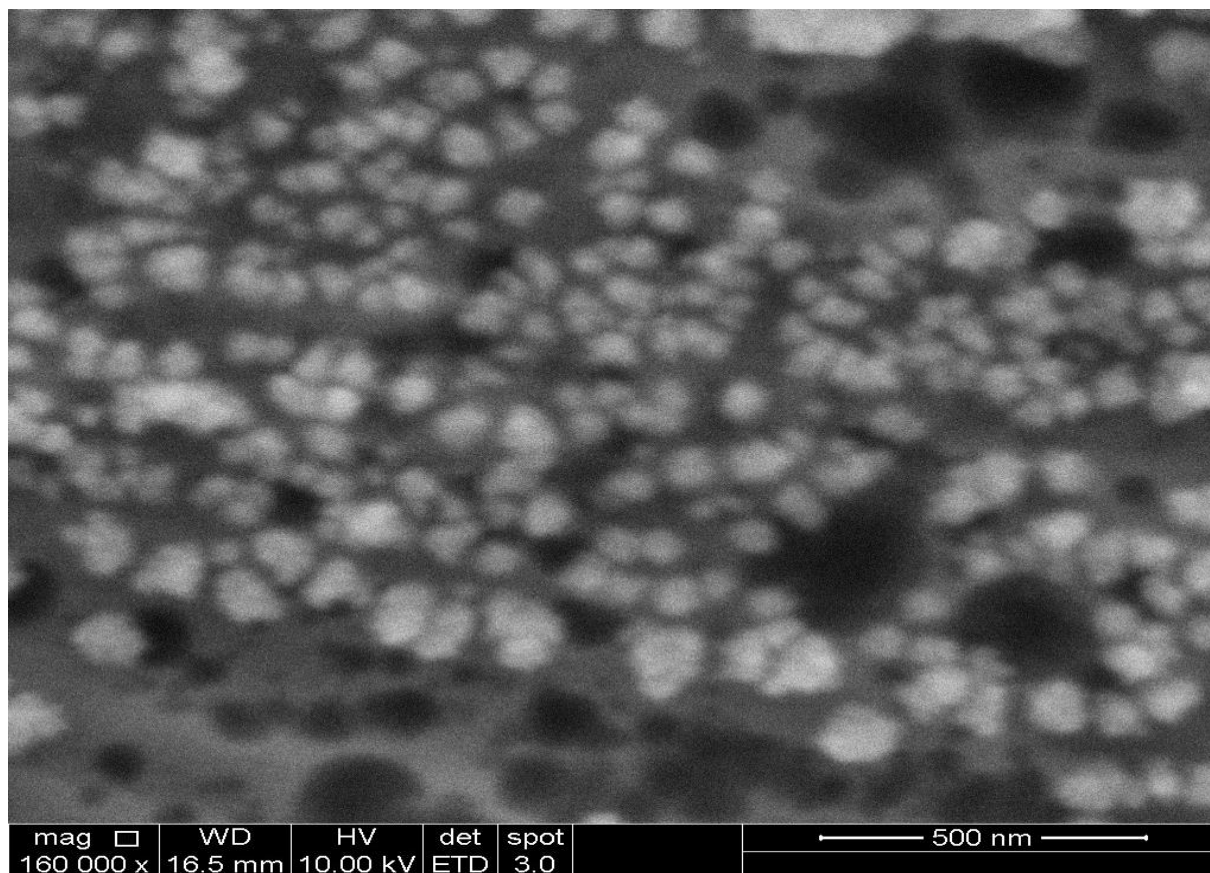


**Figure 2.** SEM micrograph of deposited platinum nanostructure on tantalum electrode

To investigate the optimal deposition time for the process, several experiments were carried out in which the time of deposition was varied, while the other parameters were held constant. The prepared structures were analysed by SEM and cyclic voltammetry. Figure 3 shows the cyclic voltammogram for the platinum nanostructured electrode deposited on tantalum substrate from  $1 \times 10^{-4} \text{M}$   $\text{PtCl}_6^-$  solution. The voltammogram shows enhanced characteristic of platinum features. The cyclic voltammogram, which proves the identity of the deposited nanoparticles because it displays the features of platinum electrodes [28].

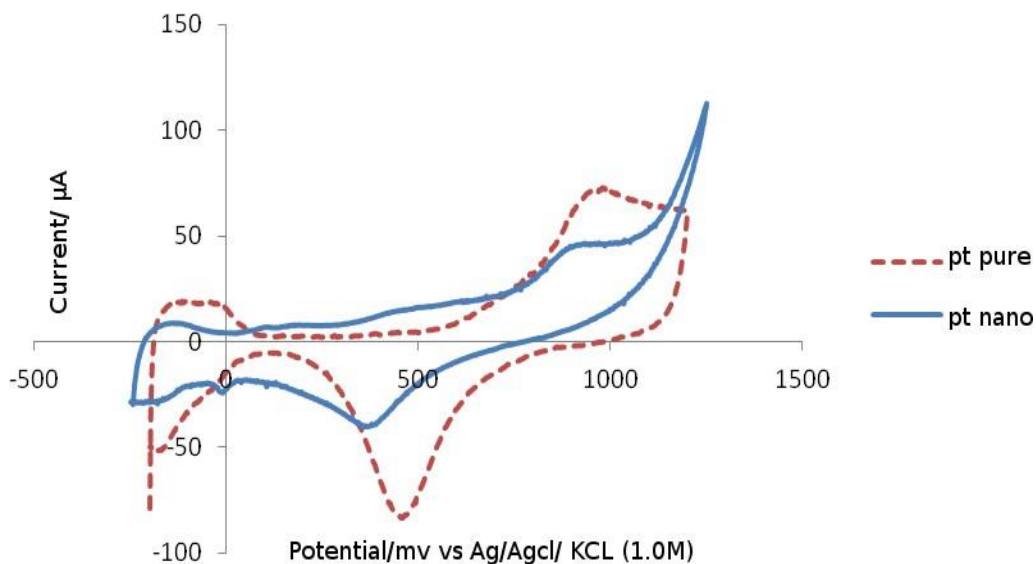


**Figure 3.** Cyclic voltammograms of a platinum nanostructure deposited on a tantalum electrode.

According to cyclic voltammetry, the platinum nanostructured electrode fabricated by deposition of platinum nanoparticles over a tantalum substrate. The presence of platinum voltammetric features is a strong evidence for deposition platinum nanoparticles. It is noticed that the maximum surface area was obtained when the frequency applied is 100 Hz. This indicates that the optimal frequency of square wave for platinum nanoparticle deposition is 100 Hz. The deposited particles shows in Figure 2 were examined by EDX spectroscopy Figure 4 proves positively the deposition of platinum nanoparticles.

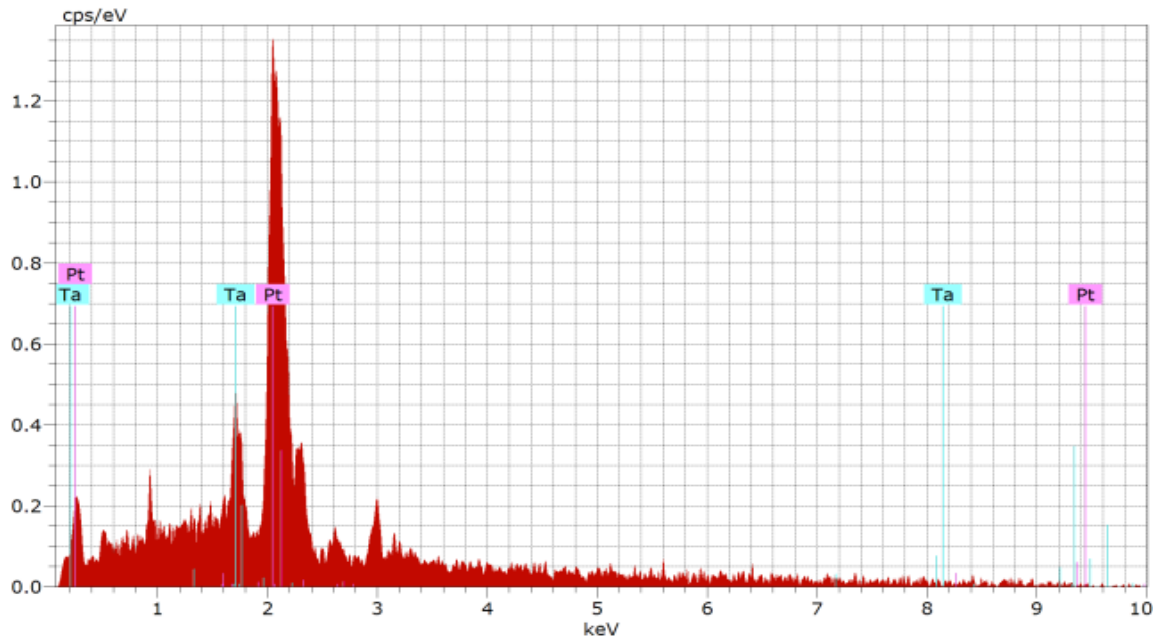


**Figure 4.** EDX spectra of platinum nanostructures deposited on tantalum electrodes

## Modification of nanostructures platinum electrodes by Iodine

Iodine was found to adsorb irreversibly on nanostructured platinum electrodes surface at open circuit. The experiments were conducted from  $10^{-2}$  M of iodine in 0.5 M  $H_2SO_4$  solution. The exposure time of the nanostructured electrode to the above- mentioned solution was 5 minutes. The Modified nanostructures platinum were analyzed by cyclic voltammetry and EDX. Figure 5 shows the voltammograms of the platinum nanostructured electrode dosed with iodine monolayer. The peak observed at 1.11V is attributed to irreversibly adsorbed iodine monolayer.

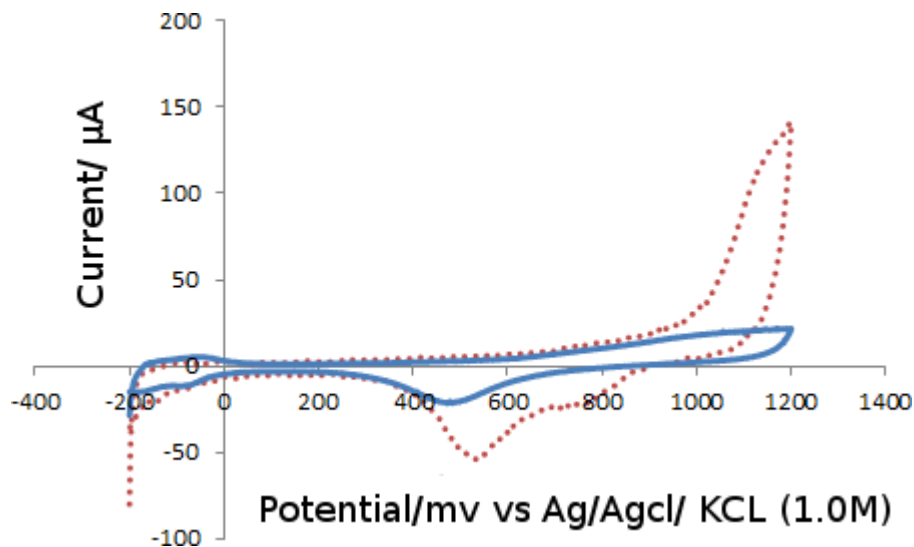


**Figure 5.** Cyclic voltammograms of platinum nanostructures electrodes modified by iodine ( ----) platinum nanostructure on tantalum electrode (—).

The iodine-coated platinum nanoparticle electrode voltammograms recorded in 0.5 M  $H_2SO_4$  (dashed line) superposed on cyclic voltammograms of a bread platinum electrode nanoparticle (solid line). The absence of any redox activity, especially the adsorption of oxygen and hydrogen between the limit on hydrogen evolution (around -0.2 V) and the threshold for surface iodine desorption (around 0.95 V) shows almost total suppression of surface treatments. It is obvious that iodine is partially desorbed from the surface when the potential for the platinum-coated electrode is scanned beyond 0.95 V. Again, restoring surface cleanliness requires a large number of potential cycles, combined with frequent rinsing of the working electrode and its compartment, between hydrogen and oxygen evolution limitations. The iodine-coated platinum nanoparticle electrode's electrochemical sensors are expressed through a picking focused at 1.18 V. However, the iodine monolayer is stable as long as the potential of the electrodes does not exceed 0.95 V. Therefore, usually between -0.1 and 0.95 volts are a useful range for analytical purposes. Figure 6 shows the EDX spectrum for a nanostructured platinum surface with iodine. The identity of the platinum and iodine is proved by the specific peaks observed at 1.6, 2 and 4.1 Kev.

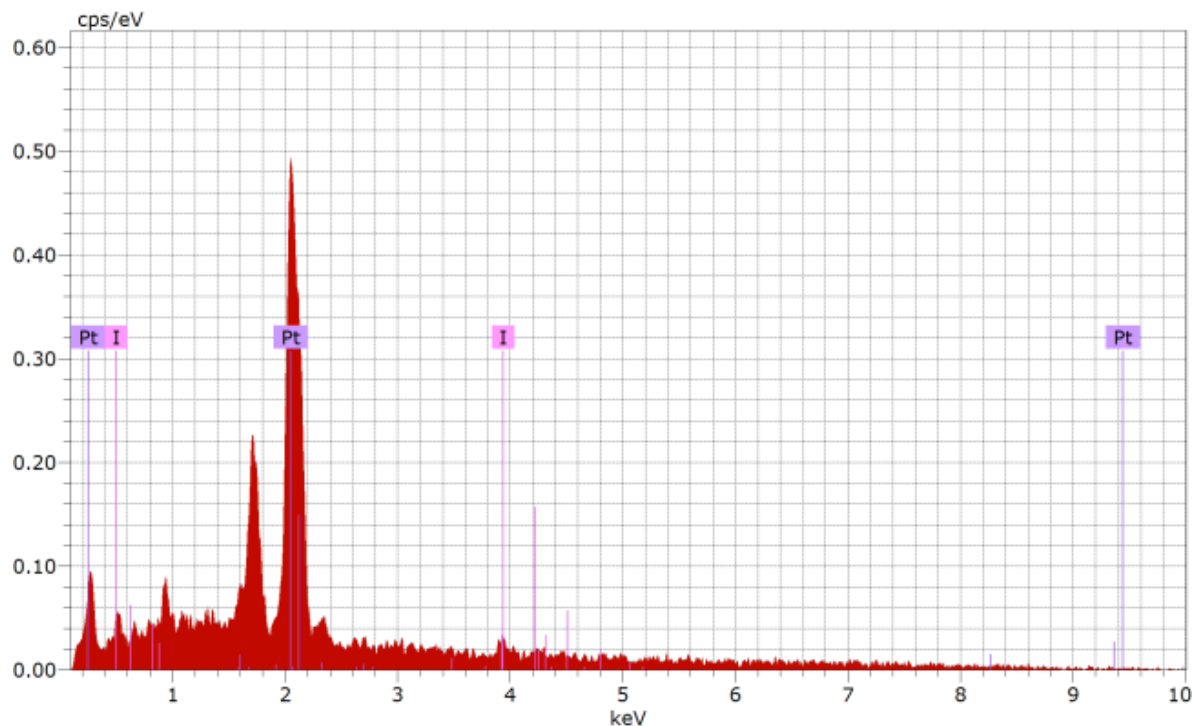


**Figure 6.** EDX spectra of deposited nanostructures platinum electrodes on tantalum by iodine

Figure 7 shows the cyclic voltammograms for the platinum nanoparticle electrode with iodine atoms in 0.5 M  $H_2SO_4$ , recorded at different scan rates.

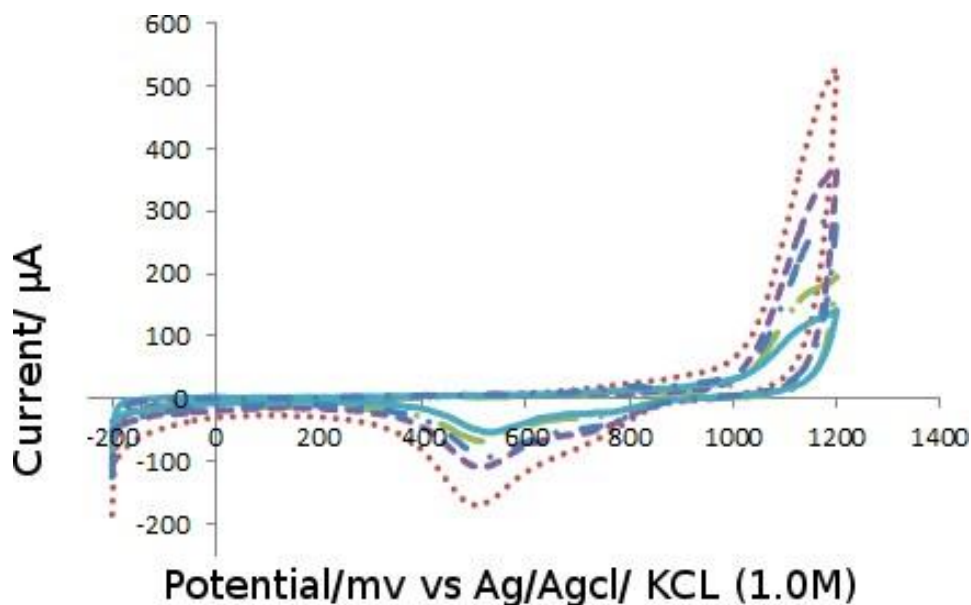


**Figure 7.** Cyclic voltammogram adsorbed of iodine on platinum nanostructure on tantalum electrode (... ) scan rate 100 mv/s (---- ) scan rate 50 mv/s (— ) scan rate 25 mv/s.

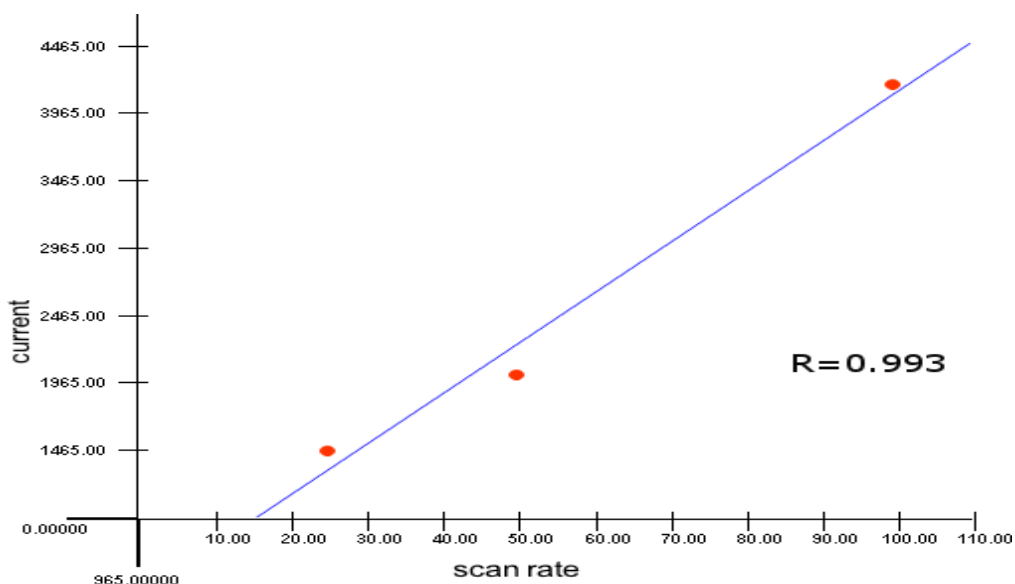
The platinum nanoparticle electrode modified by iodine is sufficiently stable to survive rinsing with the electrolytes supported and electrode cyclization potential in the potential range less than the iodine oxidation threshold potential. The major contribution towards the residual current on the E—i trace for the iodine-coated nanoparticle electrode is the double-layer charge current, as surface faradaic activities are eliminated from the iodine-coated nanoparticle electrode. For background level determination, a voltammograms was registered in 20 different iodination experiments with the iodine-coated platinum nanoparticle electrode. In the background current, the current level shows a continuous current range between -0.1 and 0.95 V. In the background current, the current level shows a continuous current range between 0.1 and 0.95 V.

Table 1 shows the measured peaks current along with scan rates used for obtaining these voltammograms (No of rep: 3).

**Table 1.** Current peak obtained for each scan rate for I adsorbed on platinum nanostructure electrode.

Scan rate	25 mv/s	50 mv/s	100 mv/s
peak Current ( $\mu\text{A}$ )	<b>1465</b>	<b>2021</b>	<b>4157</b>

Figure 8 shows a plot for the peaks current versus the scan rate. A linear relationship between the scan rate and the peaks current indicate that these atoms are at the surface rather than in the bulk solution.

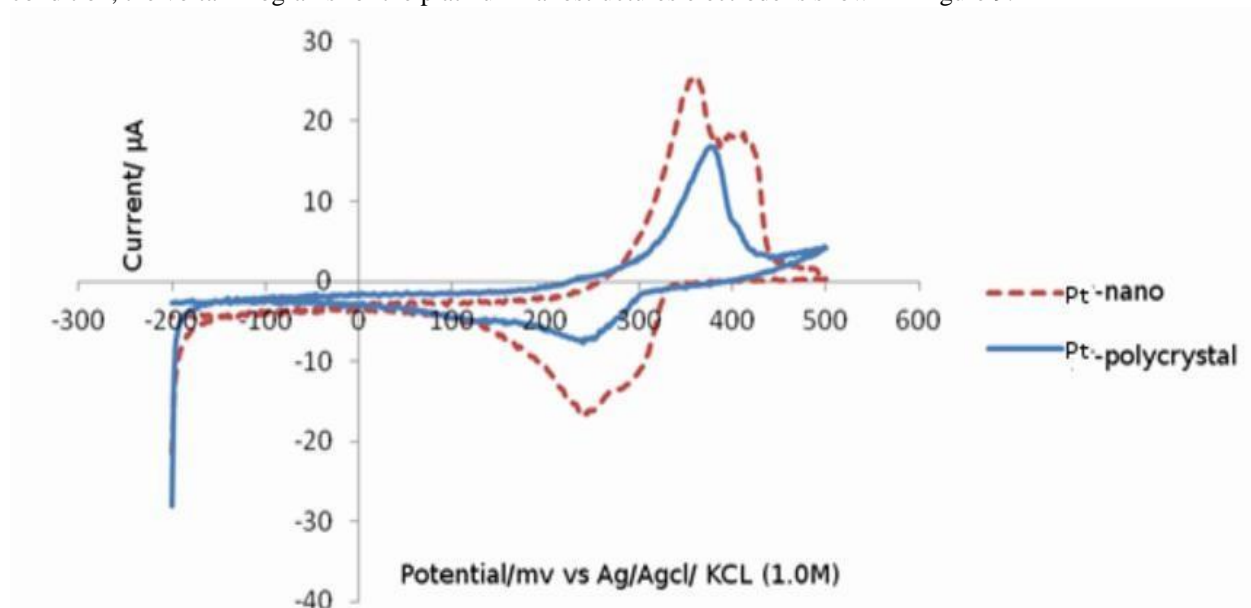


**Figure 8.** A plot of anodic peak current ( $I_p$ ) against scan rate extracted from cyclic voltammograms of adsorption I- platinum nanostructure electrode in 0.5 M  $\text{H}_2\text{SO}_4$ .

### Characterization silver ion by platinum nanostructures electrode modified by iodine

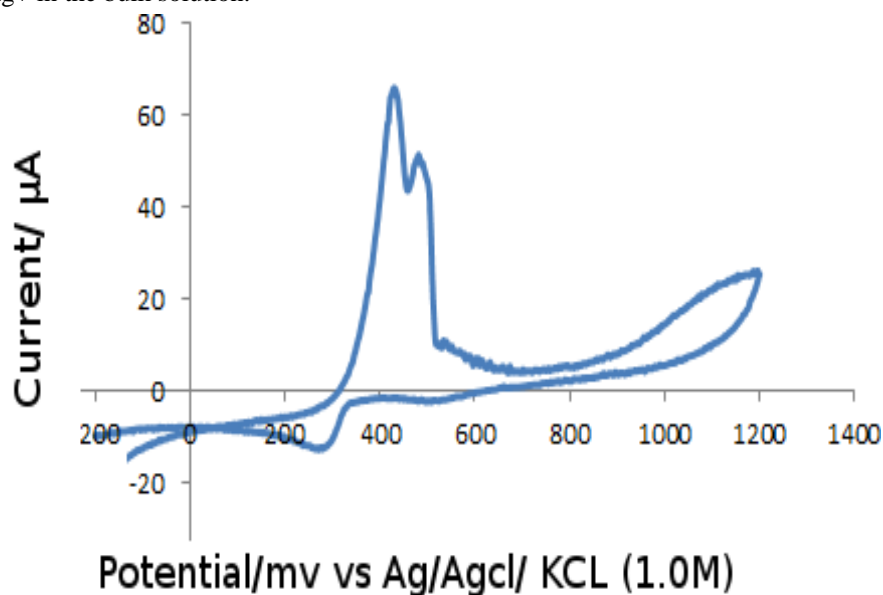
Figures 9 show two voltammograms, one recorded of platinum nanostructures electrode modified by iodine while the second was recorded on platinum nanostructures electrode. The voltammograms show different plane of surface platinum nanostructures electrode modified by iodine have two peak at 0.36 and 0.4 V but platinum nanostructures

electrode have one peak at 0.38V the reason for this sensitive surface deposition of silver. In the same experimental condition, the voltammograms for the platinum nanostructures electrode is shown in Figure 9.



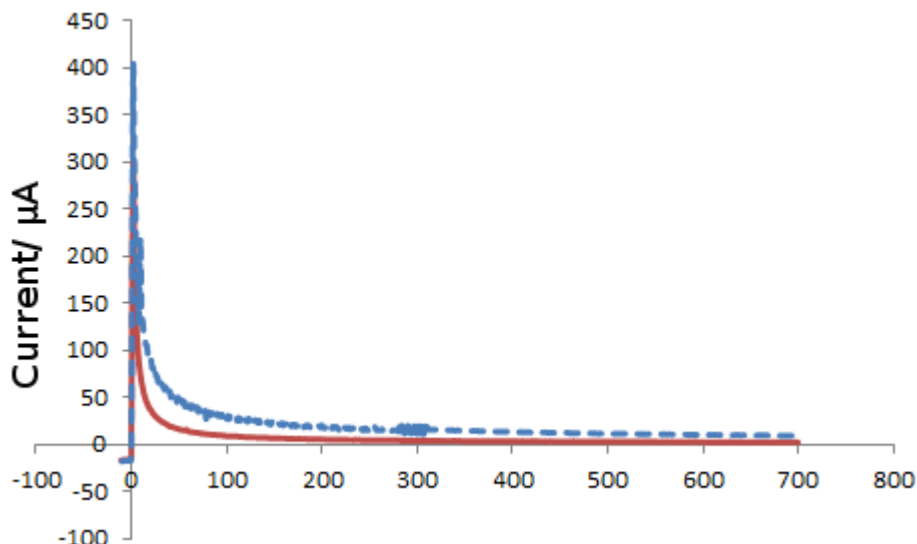
**Figure 9.** Cyclic voltammogram of platinum nanostructures electrode modified by iodine ( --- ) and platinum nanostructures electrode ( — ) of electrochemical sensors for 1 mM  $\text{Ag}^+$ .

Figure 10 shows a representative cyclic voltammograms in a solution containing 0.5 M  $\text{H}_2\text{SO}_4$  and 1 mM  $\text{Ag}^+$  for the iodine-coated platinum nanoparticle electrode. The voltammogram shows a cathodic peak for  $\text{Ag}^+$  reduction centered at 0.322 V and an anodic peak for silver stripping from the platinum surface centered at 0.480 V. The anodic peaks are significantly larger and sharper than the cathodic peak. The anodic peaks are 410 and 500 mV, while the cathodic peak is -300 mV. The anodic peak current will be used as an analytical signal to determine the concentration of  $\text{Ag}^+$  in the bulk solution.



**Figure 10.** Cyclic voltammogram of iodine-coated platinum nanoparticle electrode in a solution containing 0.5 M  $\text{H}_2\text{SO}_4$  and 1m M  $\text{Ag}^+$ .

When the silver stripping peak on the iodine-coated electrode was compared to that on the iodine-modified platinum electrode, the following observations can be made: The area beneath the anodic peak of the iodine-coated electrode is slightly larger than that of the bare platinum electrode, and the anodic peak currents and widths of the two electrodes differ. Figure 11 shows Chronoamperogram of 1m M Ag<sup>+</sup> on nanostructures platinum modified by iodine. The Chronoamperogram stepped potential and measure current.



**Figure 11.** Chronoamperogram of 1m M Ag<sup>+</sup> on nanostructured platinum electrode modified by iodine in 0.5 M H<sub>2</sub>SO<sub>4</sub>.

## Conclusion

Deposition parameters affect greatly the size, shape and distribution of the deposited nanoparticles and this is proved by SEM and cyclic voltammetry. Parameters for deposition were investigated to explore the optimal deposition parameters that were determined based on SEM images that show the desired spherical geometry and the smallest particle size with uniform distribution on the electrode surface. The new nanostructured electrode have unique properties due to their high surface to volume ratio that enhances their electrochemical activity. The new modified electrode could be utilized as electrochemical sensors due to their high electroactive and high electrochemical sensors surface area that increase their sensitivity. Modified of the nanostructured platinum electrode surface was carried out by dipping the electrode into a solution, which contains the cation of the element Open-circuit. The electrochemical sensors of the modified electrode had been tested towards the determination of silver ion. The voltammograms attests that the new electrode modified by iodine has higher electrochemical sensors surface than the substrate.

## References

- [1] Akbar, S., Anwar, A., & Kanwal, Q. (2016). Electrochemical determination of folic acid: A short review. *Analytical Biochemistry*, 510, 98-105. doi:10.1016/j.ab.2016.07.002
- [2] Liu, Y., Li, X., Chen, J., & Yuan, C. (2020). Micro/Nano electrode ARRAY sensors: Advances in fabrication and EMERGING applications in bioanalysis. *Frontiers in Chemistry*, 8. doi:10.3389/fchem.2020.573865

- [3] Ren, L., Jiang, Q., Chen, K., Chen, Z., Pan, C., & Jiang, L. (2016). Fabrication of a micro-needle array electrode by thermal drawing for bio-signals monitoring. *Sensors*, 16(6), 908. doi:10.3390/s16060908
- [4] Alkhaldeh, A., & Alkhaldeh, R. (2020). Highly sensitive COPPER heavy METAL analysis On Nanoparticle platinum and Palladium electrode. *International Journal of Engineering and Artificial Intelligence*, 1(2), 33-39. doi:10.20944/preprints202005.0069.v1
- [5] Nazemi, H., Joseph, A., Park, J., & Emadi, A. (2019). Advanced micro- and NANO-GAS Sensor technology: A review. *Sensors*, 19(6), 1285. doi:10.3390/s19061285
- [6] Walker, N. L., & Dick, J. E. (2021). Oxidase-loaded hydrogels for versatile potentiometric metabolite sensing. *Biosensors and Bioelectronics*, 178, 112997. doi:10.1016/j.bios.2021.112997
- [7] Alkhaldeh, A. (2020). Analytics of antimony in natural water of nanoparticle platinum electrode by application square wave voltammetry. *International Journal of Multidisciplinary Sciences and Advanced Technology*, 1(4), 96-103. doi:10.20944/preprints202005.0072.v1
- [8] Manciu, F. S., Oh, Y., Barath, A., Rusheen, A. E., Kouzani, A. Z., Hodges, D., Bennet, K. E. (2019). Analysis of CARBON-BASED Microelectrodes for Neurochemical sensing. *Materials*, 12(19), 3186. doi:10.3390/ma12193186.
- [9] Mierzejewski, M., Steins, H., Kshirsagar, P., & Jones, P. D. (2020). The noise and impedance of microelectrodes. *Journal of Neural Engineering*, 17(5), 052001. doi:10.1088/1741-2552/abb3b4.
- [10] Hay, C. E., Lee, J., & Silvester, D. S. (2019). Formation of 3-dimensional gold, copper and palladium microelectrode arrays for enhanced electrochemical sensing applications. *Nanomaterials*, 9(8), 1170. doi:10.3390/nano9081170.
- [11] Krishan, M., Alkhaldeh, A., & Soliman, A. (2020). Development of nitride-sensors for monitoring in control systems. *Journal of Measurements in Engineering*, 8(3), 90-97. doi:10.21595/jme.2020.21384.
- [12] Krasovska, M., Gerbreder, V., Mihailova, I., Ogurcovs, A., Sledzskis, E., Gerbreder, A., & Sarajevs, P. (2018). ZnO-nanostructure-based electrochemical sensor: Effect of nanostructure morphology on the sensing of heavy metal ions. *Beilstein Journal of Nanotechnology*, 9, 2421-2431. doi:10.3762/bjnano.9.227.
- [13] Kanoun, O., Müller, C., Benchirouf, A., Sanli, A., Dinh, T., Al-Hamry, A., Bouhamed, A. (2014). Flexible carbon nanotube films for high performance strain sensors. *Sensors*, 14(6), 10042-10071. doi:10.3390/s140610042
- [14] Beitollahi, H., Tajik, S., GarkaniNejad, F., & Safaei, M. (2020). Recent advances in ZnO nanostructure-based electrochemical sensors and biosensors. *Journal of Materials Chemistry B*, 8(27), 5826-5844. doi:10.1039/d0tb00569j
- [15] Cho, I., Kim, D. H., & Park, S. (2020). Electrochemical biosensors: Perspective on functional nanomaterials for on-site analysis. *Biomaterials Research*, 24(1). doi:10.1186/s40824-019-0181-y
- [16] Yu, L., Kim, B., & Meng, E. (2014). Chronically implanted pressure sensors: Challenges and state of the field. *Sensors*, 14(11), 20620-20644. doi:10.3390/s141120620

- [17] Alkhalwaldeh, A. K. (2020). Platinum nanoparticle in Tantalum Electrode for the ELECTROCHEMICAL analysis of heavy metal IONS formed by the ion BEAM Sputtering Deposition. *International Journal of Intelligent Computing and Technology*, 4(1), 25-35. doi:10.20944/preprints202006.0179.v1
- [18] Cha, K. H., & Meyerhoff, M. E. (2017). Compatibility of nitric Oxide release with Implantable Enzymatic GLUCOSE sensors based on Osmium (III/II) Mediated Electrochemistry. *ACS Sensors*, 2(9), 1262-1266. doi:10.1021/acssensors.7b00430
- [19] Ricci, P. P., & Gregory, O. J. (2021). Free-standing, thin-film sensors for the trace detection of explosives. *Scientific Reports*, 11(1). doi:10.1038/s41598-021-86077-6
- [20] Mistry, K. K., Layek, K., Mahapatra, A., RoyChaudhuri, C., & Saha, H. (2014). A review on amperometric-type immunosensors based on screen-printed electrodes. *The Analyst*, 139(10), 2289. doi:10.1039/c3an02050a
- [21] Costa-Rama, E., & Fernández-Abedul, M. T. (2021). Paper-based screen-printed electrodes: A new generation of low-cost electroanalytical platforms. *Biosensors*, 11(2), 51. doi:10.3390/bios11020051
- [22] Purcell, E., Becker, M., Guo, Y., Hara, S., Ludwig, K., McKinney, C., Li, W. (2021). Next-Generation diamond electrodes for Neurochemical Sensing: Challenges and opportunities. *Micromachines*, 12(2), 128. doi:10.3390/mi12020128
- [23] Alkhalwaldeh, A. K. (2021). Platinum nanoparticle electrode electro-chemical lead (ii) determination with square-wave voltammetry modified with iodine. *PROCEEDINGS OF GREEN DESIGN AND MANUFACTURE 2020*, 1(1), 035. doi:10.1063/5.0045328
- [24] Alkhalwaldeh, A. K. (2020). Platinum nanoparticle electrode modified iodine used cyclic voltammetry and chronoamperometric for determination of ascorbic acid. *Analytical and Bioanalytical Electrochemistry*, 12(6), 780-792. doi:10.1063/5.0045328
- [25] Lin, W., Brondum, K., Monroe, C., & Burns, M. (2017). Multifunctional water sensors for PH, ORP, and Conductivity using Onlymicrofabricated PLATINUM ELECTRODES. *Sensors*, 17(7), 1655. doi:10.3390/s17071655
- [26] Koklu, A., Sabuncu, A. C., & Beskok, A. (2016). Rough gold electrodes for Decreasing impedance at The Electrolyte/Electrode Interface. *ElectrochimicaActa*, 205, 215-225. doi:10.1016/j.electacta.2016.04.048
- [27] Alkhalwaldeh, A. (2020). Electrochemical Analysis of Heavy Metal by Cyclic Voltammetry Method. *International Journal of Engineering and Artificial Intelligence*, 2(2), 27-33. doi:10.20944
- [28] Alkhalwaldeh, A. (2020). Platinum Nanoparticles for the Electrochemical Study of Heavy Metal Ions Formed by the Sputtering Deposition of the Ion Beam Electrode. *International Journal of Engineering and Artificial Intelligence*, 1(3), 1-8.